

Identification of a Region Involved in the Communication between the NADP(H) Binding Domain and the Membrane Domain in Proton Pumping *E. coli* Transhydrogenase[†]

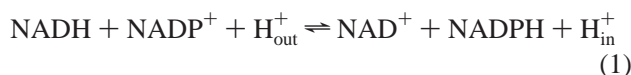
Magnus Althage, Tania Bizouarn,[‡] and Jan Rydstrom*

Department of Biochemistry and Biophysics, Göteborg University, S-413 90 Göteborg, Sweden

Received February 14, 2001; Revised Manuscript Received May 22, 2001

ABSTRACT: The two hydrophilic domains I and III of *Escherichia coli* transhydrogenase containing the binding sites for NAD(H) and NADP(H), respectively, are located on the cytosolic side of the membrane, whereas the hydrophobic domain II is composed of 13 transmembrane α -helices, and is responsible for proton transport. In the present investigation the segment β C260– β S266 connecting domain II and III was characterized primarily because of its assumed role in the bioenergetic coupling of the transhydrogenase reaction. Each residue of this segment was replaced by a cysteine in a cysteine-free background, and the mutated proteins analyzed. Except for β S266C, binding studies of the fluorescent maleimide derivative MIANS to each cysteine in the β C260– β R266 region revealed an increased accessibility in the presence of NADP(H) bound to domain III; an opposite effect was observed for β S266. A β D213– β R265 double cysteine mutant was isolated in a predominantly oxidized form, suggesting that the corresponding residues in the wild-type enzyme are closely located and form a salt bridge. The β S260C, β K261C, β A262C, β M263, and β N264 mutants showed a pronounced inhibition of proton-coupled reactions. Likewise, several β R265 mutants and the D213C mutant showed inhibited proton-coupled reactions but also markedly increased K_m^{NADPH} values. It is concluded that the mobile hinge region β C260– β S266 and the β D213– β R265 salt bridge play a crucial role in the communication between the proton translocation/binding events in domain II and binding/release of NADP(H) in domain III.

Proton-translocating nicotinamide nucleotide transhydrogenase is a membrane bound protein found in the inner membrane of animal mitochondria and the plasma membrane of many prokaryotes, e.g., bacteria, parasites, and green algae. The enzyme participates in the bioenergetic processes of the cell and uses the electrochemical proton gradient across the membrane to drive NADPH formation from NADH according to reaction 1:



where “in” and “out” represent the cytoplasm and periplasm, respectively, in bacteria. Structural and functional analyses (1–3) reveal a tripartite structure (Figure 1). Two hydrophilic domains, i.e., domain I (dI,¹ 400 residues) and domain III (dIII, 200 residues), protrude from the membrane into the cytosol and contain the NAD(H) and NADP(H) binding sites,

respectively. The hydrophobic domain II (dII, 310 residues), contains 13 transmembrane α helices in the *Escherichia coli* enzyme and the important β H91 and β N222 residues that form part of the proton conducting pathway (3, 4). In addition to this structure–function division, the *E. coli* enzyme is composed of two subunits, the α and β subunits, containing dI and dIII (5), respectively. Also, 4 of the 13 transmembrane α -helices reside in the α subunit and 9 in the β subunit (Figure 1). dI of *Rhodospirillum rubrum* is expressed as a separate subunit, which can be readily and reversibly removed from the intact enzyme (6, 7).

Structure–function studies of the isolated extra membranous dI and dIII (6–9) revealed that, in the absence of dII, these domains are unable to catalyze reaction 1 in a manner characteristic of the wild-type enzyme. However, they catalyze a fast so-called cyclic reaction mediated by NADP(H) bound to dIII, which is assumed to be limited mainly by the hydride equivalent transfer step. The role of the transmembrane helices constituting dII is therefore not only to transport protons through the membrane but also to energetically couple this transport to the physiologically relevant production of NADPH, probably through a binding change mechanism in dIII (3, 10, 11), somewhat analogous to the interaction between F_1 and F_0 in the F_1F_0 -ATP synthase system (12).

Several regions may be potentially involved in the transmission of information from the protonation site(s) in dII to the NADP(H)-binding site in dIII. The region linking dI to the first helix (residues α 380– α 402), as well as the

[†] This work was supported by the Swedish Natural Science Research Council.

* To whom correspondence should be addressed. Phone: +46 31 7733921. Fax: +46 31 7733910. E-mail: jan.rydstrom@bcbp.gu.se.

[‡] Present address, CGM, CNRS, GIF/Yvette, France.

¹ Abbreviations: CfTH, cysteine-free intact transhydrogenase; wtTH, wild-type intact transhydrogenase; AcPyAD⁺, 3-acetyl pyridine NAD⁺; dI, dII, dIII, domain I, domain II, and domain III, respectively, of transhydrogenase; rrl, domain I of *Rhodospirillum rubrum* transhydrogenase; NEM, *N*-ethylmaleimide; MIANS, 2-(4-maleimidylanilino)-naphthalene-6-sulfonic acid; ACMA, 9-amino-6-chloro-2-methoxyacridine.

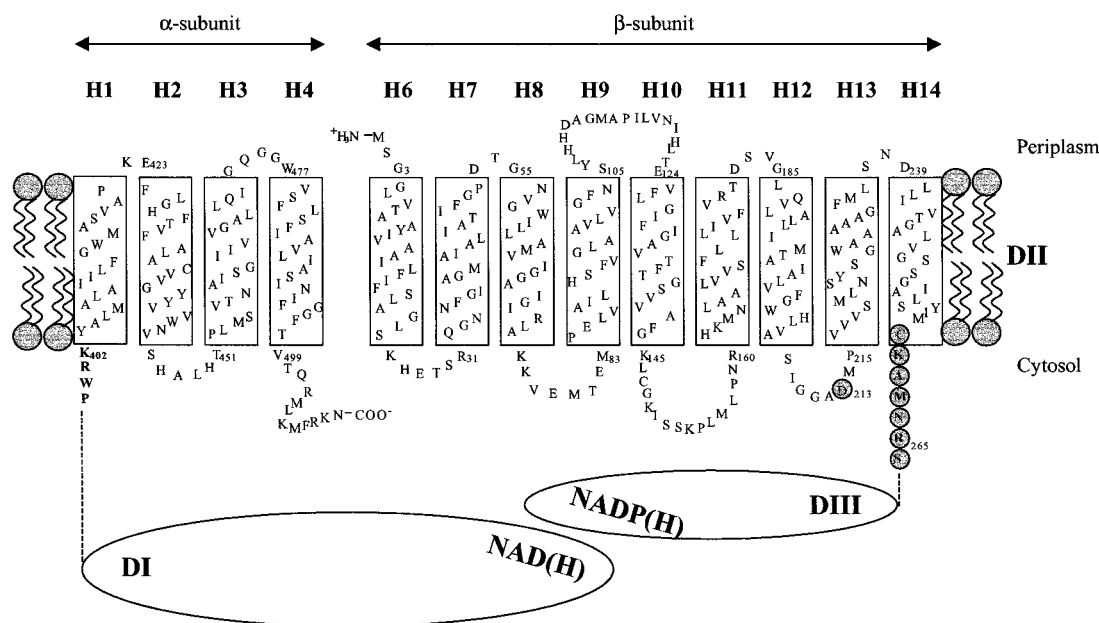


FIGURE 1: Membrane topology of the *E. coli* transhydrogenase. The membrane topology of domain II has been depicted according to Mueller et al. (4). Mutated positions are marked with gray and circled. The numbering of the α -helices (4) and the location of the α (54 kDa) and β (48 kDa) subunits are indicated above the sequence. The two hydrophilic domains facing the cytosol are indicated as DI and DIII below the sequence.

first helix (residues $\alpha 403$ – $\alpha 421$) are poorly conserved, and not always present among the different transhydrogenases sequences available. Hence, it seems unlikely that they play a role in the coupling process. For similar reasons, and also due to their very short length (see Figure 1), the periplasmic loops do not seem to contain any important motifs. Extensive mutagenesis experiments have been carried out on most of the conserved residues located in the cytoplasmic loops (1, 13, 14). These studies showed that residue $\beta D213$ and probably $\beta H450$ are particularly important (13, 14). Residue $\beta R265$ has earlier been shown to adopt different conformations in the absence and presence of NADP(H) (15). The 209–266 region is strongly conserved. However, although there are indications that this region is important (16), a functional role of residues $\beta 260$ – $\beta 266$, including the trypsin-sensitive $\beta R265$, in linking dII and dIII, has not been systematically investigated previously.

In the present investigation, the recently produced cysteine-free *E. coli* H^+ -transhydrogenase (17) has made it possible to characterize the role of the $\beta 260$ – $\beta 266$ region by cysteine mutagenesis and the relationship between residues 213 and 265. The results suggest that this region indeed has a functional role in the bioenergetic coupling of the enzyme.

MATERIALS AND METHODS

Site-Directed Mutagenesis. The plasmid PCLNH contains the gene coding for the cysteine-free transhydrogenase (cfTH) to which a six residue long N-terminal histidine tag has been attached (4). This plasmid was used as template for the single cysteine mutants (since the β subunit was the target in all mutants, the prefix β has been omitted in all mutants), i.e., cfS260C, cfK261C, cfA262C, cfM263C, cfN264C, cfR265C, cfS266C, and cfD213C, as well as the double mutant cfD213C–R265C. The second plasmid used, called PNHIS, contains the gene coding for the wild-type transhydrogenase (wtTH) to which had been attached a

histidine tag (4). PNHIS was used for the construction of the three single mutants, wtR265A, wtR265K, and wtR265E. These 12 mutants were all produced using the Quikchange mutagenesis kit (Stratagene); the protocol provided with the kit was followed without any modifications. All primers were supplied by Medprobe (Norway). Full-length genes were sequenced to verify the correctness of all mutant products.

Expression and Purification of Enzymes. Expression and purification of cfTH, wtTH and the mutants were performed as described (18). Expression and purification of *R. rubrum* domain I (rri) was performed as described (19). All enzymes were analyzed by SDS–PAGE using 10–20% tris-glycine gels (Novex, Germany).

Determination of Protein Concentrations. Protein concentrations were determined by the bicinchoninic acid assay (BCA) using BSA as standard (20).

Determination of NADP(H) Content by Fluorescence. Bound NADPH was analyzed by measuring its fluorescence at the excitation wavelength 340 nm and the emission wavelength 460 nm on a SPEX model FL1T1 $\tau 2$ spectrofluorometer. The amount of bound NADPH was determined by its oxidation by 2 mM oxidized glutathione and 5 units glutathione reductase using the same MOPS buffer as above. Bound NADP⁺ was estimated by its reduction by 1 unit isocitrate dehydrogenase and 2 mM isocitrate in a buffer containing 20 mM MOPS (pH 7.0), 5 mM MgCl₂ and 0.01% Brij.

Activity Assays. To characterize the kinetic and thermodynamic properties of the different mutants studied, two different transhydrogenase activities were determined. The reverse activity was assayed as reduction of 400 μ M of the NAD⁺ analogue acetyl-pyridine adenine dinucleotide (AcPyAD⁺) by 400 μ M NADPH in buffer A (20 mM Mes, 20 mM Hepes, 20 mM Ches and 20 mM Tris, 50 mM NaCl, and 0.01% Brij 35, adjusted to pH 7.0). The cyclic reaction was estimated by the reduction of 400 μ M AcPyAD⁺ by

200 μM NADH in the presence/absence of 200 μM NADP⁺ or NADPH in buffer B (20 mM Mes, 20 mM Hepes, 20 mM Ches and 20 mM Tris, 50 mM NaCl, 0.01% Brij 35 supplemented with 1 mM EDTA and 2 mM MgCl₂, adjusted to pH 6.0) (21, 22). The cyclic reaction in the presence and absence of rrI was assayed under the same conditions. Both the reverse and cyclic reactions were analyzed at 375 nm, at 25 °C, using the absorption coefficient 6100 M⁻¹ cm⁻¹.

The pH dependencies of the reverse and cyclic reactions were investigated by carrying out these reactions at different pH (5.0–8.5). The pH of the above buffers was adjusted by the addition of HCl/NaOH.

MgCl₂ Dependence of the Reverse Reaction. The reverse reaction was performed in the presence of various concentrations of MgCl₂ and at different pH. To observe the full effect of Mg²⁺ it was necessary to omit NaCl from the buffer.

Preparation of Proteoliposomes. Proteoliposomes were prepared as described (17) with the following modification; after the liposomes had been prepared by sonication in 100 mM potassium phosphate (pH 7.2), the dialysis step was omitted. All transhydrogenases tested were reconstituted in liposomes under identical conditions.

Proton Pumping Activity. The ability of the transhydrogenases to translocate protons from the outside to the inside of the vesicles was estimated by following the quenching of 9-amino-6-chloro-2-methoxyacridine (ACMA) fluorescence at 475 nm (excitation wavelength 415 nm) (23). Proteoliposomes were mixed with 1 μM ACMA and 400 μM NADPH in buffer A supplemented with 50 mM KCl and 5 mM MgCl₂ at room temperature. The reaction was initiated by the addition of 400 μM AcPyAD⁺. After the fluorescence signal had stabilized, 2 μM CCCP was added to dissipate the pH gradient. All proteoliposomes were produced on the same day and under the same conditions.

MIANS Binding Measured by Fluorescence. When MIANS interacts with sulfhydryl groups it becomes fluorescent. This reaction was monitored by a SPEX Model FL1T1 τ 2 spectrofluorometer. Excitation and emission wavelengths were set to 330 and 418 nm, respectively. Excitation and emission slits were both adjusted to 4.3 nm. The absorbance in all samples was measured at 330 and 418 nm in order to estimate and adjust for the inner-filter effect as described by Kubista et al. (24). A fresh stock-solution of 10 mM MIANS prepared in 50% methanol was used each time; MeOH alone had no effect. The concentration of MIANS was determined spectrophotometrically at 322 nm using an absorption coefficient of 17 000 M⁻¹ cm⁻¹. All experiments were performed in buffer A, at 25 °C and under stirring conditions. The reactions were initiated by the addition of 4 μM MIANS. When indicated, 1 mM NADP⁺ or 100 μM NADPH was added 5 min prior to the addition of MIANS.

Semiquantitative measurements of MIANS binding to transhydrogenase by SDS–PAGE was carried out as follows. Purified transhydrogenase (20 μg) was incubated with 4 μM MIANS for 30 min in buffer A. When NADP(H) was present, it was added 5 min prior to the addition of MIANS. After 30 min, a 50-fold excess of cysteine was added in order to block residual unreacted MIANS. Equal parts of sample and SDS-buffer (tris-glycine-SDS sample buffer (2 \times) (Novex) + 5% β -mercaptoethanol) were mixed, of which 15 μg protein was loaded on 10–20% Tris-glycine polyacrylamide

gels (Novex, Germany). Following the run, the gel was soaked in a solution containing 50% MeOH and 10% HAc for 1 h. A video-photograph of the gel was taken under UV-light illumination and this picture was then scanned and inverted. Coomassie Blue was added after which the gel was scanned directly.

Inhibition of the Reverse and Cyclic Reactions NEM and MIANS. The irreversible inhibition by MIANS or NEM of the activities catalyzed by the cfR265C mutant was monitored by assaying the reverse and cyclic activities of aliquots taken after 1 h of incubation of about 100 nM enzyme with 100 μM NEM or 4 μM MIANS, in the presence/absence of 400 μM NADPH. Reverse and cyclic activities were followed as described previously.

RESULTS

Single and Double Mutations Introduced into Wild-Type and Cysteine-Free Intact *E. coli* Transhydrogenases. The cysteine mutants cfS260C, cfK261C, cfA262C, cfM263C, cfN264C, cfR265C, and cfS266C were produced in order to investigate the altered accessibility of the 260–266 region to sulfhydryl specific probes induced by the binding of NADP(H) to dIII. These residues are all located in the region linking dII and dIII (cf. Figure 1). The mutants were constructed in the cysteine-free transhydrogenase (cfTH), expressed and purified as described in the Materials and Methods. The cfS266C mutant was chosen in order to create a site close to residue R265 with minimal perturbation of the properties of the enzyme. To investigate the potential relationship between D213 and R265, the cfD213C and the cfD213C–R265C double mutants were also produced in the cysteine-free background. At position R265 three additional mutations, wtR265A, wtR265K, and wtR265E, were introduced in the wild-type transhydrogenase (wtTH), according to the same protocol as the other mutations. The purpose of these three latter mutations were to allow a more thorough investigation of this important residue which has been identified as a cleavage site for trypsin in the presence of NADP(H) (15).

Effects on the Reverse Reaction and K_m^{NADPH} . In the reverse reaction, AcPyAD⁺ is reduced by NADPH which is coupled to the transfer of a proton from the cytosol to the periplasmic space (2, 3). This reaction corresponds to reaction 1 from right to left. The reverse and cyclic activities of the different mutants are shown in Table 1. As described earlier (17), the replacements of the seven native cysteines in order to create cfTH, had little effect on activities but led to a 3-fold decrease of the K_m^{NADPH} value. As compared to cfTH, all single mutants produced in the present investigation displayed decreased reverse activities. As compared to the wild-type enzyme the same effect was found for the wtR265 mutants. However, the cfK261C to cfR265C mutants showed a reverse activity of less than 10% as compared to cfTH, whereas the cfS260C and cfS266C mutants were more active, i.e., 23–70% of wild-type activity. Furthermore, a mild change such as replacing the Arg at position R265 to a Lys led to a significant inhibition of the enzyme.

The cfD213C mutant was essentially inactive with regard to the reverse reaction; K_m^{NADPH} was increased about 3-fold (Table 1). Thus, the properties of this mutant were reminiscent of those of the cfR265C. The properties of the double

Table 1: Kinetic Parameters of Purified CfTH, wtTH and Various Mutants in These Backgrounds^a

enzyme	K_m^{NADPH} (μM)	reverse activity ($\mu\text{mol min}^{-1} \text{mg}^{-1}$)	cyclic activity without rrI ($\mu\text{mol min}^{-1} \text{mg}^{-1}$)			cyclic activity with rrI ($\mu\text{mol min}^{-1} \text{mg}^{-1}$)	
			(–NADP(H))	(+NADP ⁺)	(+NADPH)	(+NADP ⁺)	(+NADPH)
cfTH	7.2	6.5	5	31.5	28	37	39
cfS260C	6.5	1.5	3	15	12	29	24
cfK261C	3.0	0.5	3	12	10	29	23
cfA262C	4.0	0.5	10	20	20	34	26
cfM263C	4.5	0.3	5	14	12	28	28
cfN264C	5.1	0.6	4	11	12	29	22
cfR265C	17.5	0.5	17	30	27	31	33
cfS266C	5.3	4.5	12	28	25	46	43
cfD213C	24.5	0.2	nd	13	16	nd	nd
cfD213C–R265C	nd ^b	0.3	nd	10	12	nd	nd
wtTH	19.6	8.5	0.5	25	30	40	50
wtR265A	12.5	1.7	9	33	48	38	53
wtR265E	20.6	0.7	8	22	29	34	39
wtR265K	18.8	2.9	4	32	40	35	50

^a The cyclic activities have been assayed in the presence and absence of NADP(H) and rrI. ^b Not determined.

mutant cfD213C–R265C were similar to those of the cfD213C mutant (Table 1).

An unexpected result was that the reversal of the Cys to Ser mutation in the cfTH mutant to its original Cys in cfS260C had an inhibitory effect. Except for a 2–3-fold increase for the cfR265C, the cfD213C, and presumably the cfD213C–R265C mutant and a 2-fold decrease for the cfK261C mutant, the K_m^{NADPH} values were not significantly affected in the remaining mutants in the cysteine-free background, indicating that NADPH probably still bound to dIII in its usual conformation.

Cyclic Reactions Catalyzed by Mutants and Wild-Type Enzyme in the Presence or Absence of rrI. The cyclic reduction of AcPyAD⁺ by NADH is catalyzed by the NADP(H)-bound enzyme and occurs without a net proton transport (25, 26). To detect effects of the redox state of NADP(H), this reaction was performed in the presence of NADP⁺ or NADPH. All mutations introduced at residue R265 and S266 resulted in NADP(H)-dependent cyclic activities similar to those of the wild-type enzyme (Table 1). Cysteine mutants in the S260–N264 segment displayed activities of 35–70% of that of cfTH. Replacement of NADPH with NADP⁺ for these five mutants did not affect the activities of the mutants; the cfD213C and the cfD213C–R265C double mutants behaved similarly to the cfM263C and cfN264C mutants (Table 1).

Under certain conditions, such as low pH and low salt concentration, wtTH catalyses a cyclic reaction in the absence of NADP⁺/NADPH. In this case, the enzyme binds NAD(H) unspecifically to the NADP(H) site (21, 22). Under the conditions used in the present investigation, this reaction is normally rather low for wtTH but is significant for most of the mutants (Table 1). This cannot be attributed to tightly bound NADP(H), since no significant amount of substrate was found in any of the enzyme preparations (data not shown). It is more likely that the mutations introduced have decreased the specificity of the binding-site for NAD(P)(H), allowing NAD(H) to bind.

Domain I from *R. rubrum* (rrI), may be added to a mixture of dI and dIII from *E. coli* or the intact enzyme and then replaces the latter dI resulting in more active transhydrogenase reactions (27), the new complex being apparently much less sensitive to the configuration of the different domains (see Discussion for more details). As shown in Table 1, the

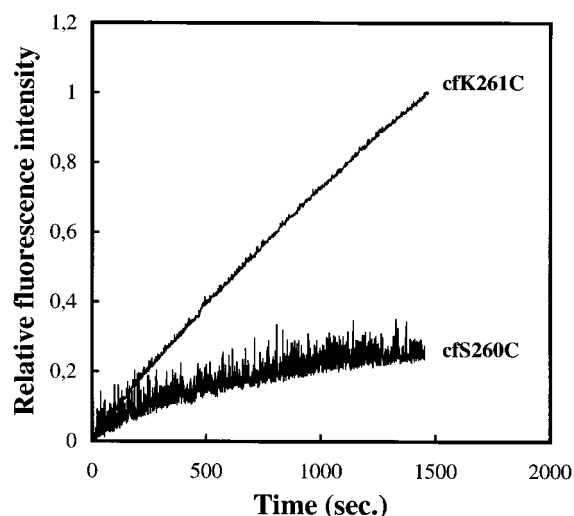


FIGURE 2: Binding of MIANS to the cfS260C and cfK261C mutants in the absence of NADP(H) monitored by fluorescence. The experiment was performed as described under Methods in 2 mL of buffer A. MIANS (4 μM) was added to initiate the reaction with 40 μg enzyme.

cyclic activities of all mutants were increased by the presence of rrI to values similar to that of the cfTH or wtTH enzyme.

Binding of MIANS to Single and Double Cysteine Mutants Monitored by Fluorescence. MIANS is a negatively charged molecule which becomes fluorescent upon reaction with sulfhydryl groups. The fluorescence of MIANS bound to a sulfhydryl is strongly enhanced by a hydrophobic environment (28–30). By following this reaction fluorometrically, the rate of binding to the proteins reflects the accessibility of the cysteine side chain to MIANS and/or its environment. However, in the experiments described below accessibility was the main determinant as judged by analysis of bound MIANS in denaturing SDS–PAGE.

Control experiments with cfTH showed a slight unspecific reactivity of MIANS with the enzyme (data not shown). As shown in Figure 2, a low rate of binding was observed for cfS260C, consistent with its localization at the membrane/solute interphase (4). In contrast, the cfK261C mutant showed a significant reaction with MIANS, or, depending on the time of reaction, some 2–5-fold higher rate as compared to cfS260C. Reaction rates for the cfA262C, cfM263C, cfN264C, and cfR265C were slightly lower but

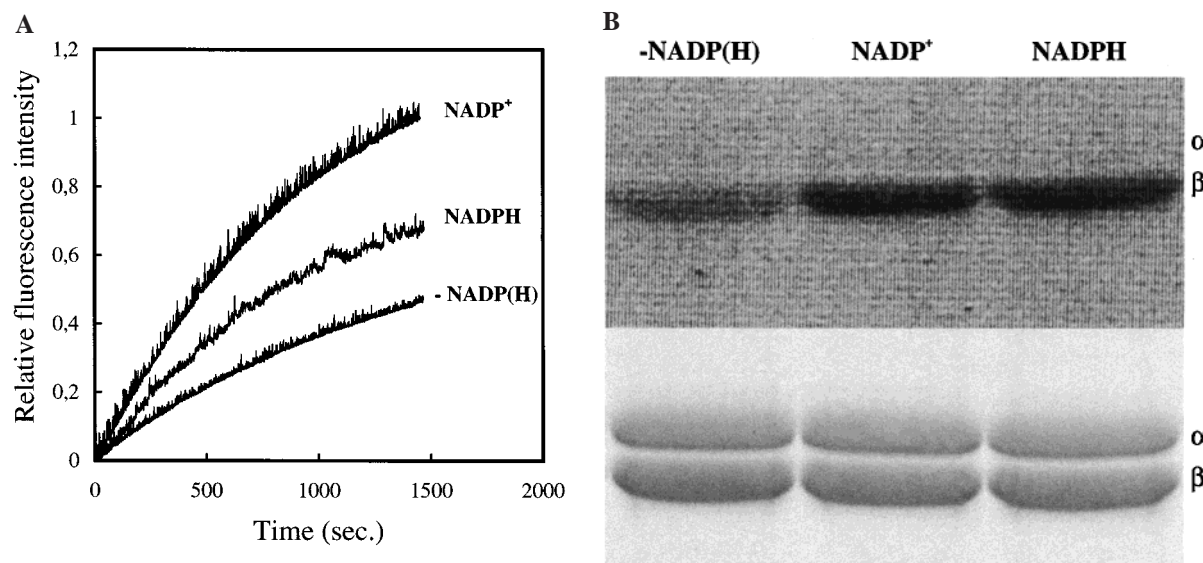


FIGURE 3: Binding of MIANS to the cfA262C mutant in the presence and absence of NADP(H) monitored by fluorescence (A) and SDS-PAGE (B). (A) The experiment was performed as described in the Materials and Methods in 2 mL of buffer A. The concentration of MIANS, NADPH, NADP^+ , and enzyme were 4 μM , 100 μM , 1.0 mM, and 20 $\mu\text{g}/\text{mL}$, respectively. The upper trace is in the presence of NADP^+ , the middle trace in the presence of NADPH and the lower trace in the absence of nucleotide. (B) The analysis was carried out by SDS-PAGE as described in the Materials and Methods. (Upper panel) MIANS fluorescence; lower panel, staining of proteins by Coomassie Blue. Additions were (upper panel, left lane) no additions; (middle lane) 1 mM NADP^+ ; (right lane) 1 mM NADPH. In both panels, the positions of the α and β subunits are indicated.

still 3–4-fold higher than that for cfS260C. The reactivities with MIANS were mirrored by an actual incorporation of MIANS in the proteins, as indicated by semiquantitative analyses on SDS-PAGE. With all mutants the reaction with MIANS led to a proportional inhibition of the catalytic activities of the enzymes (data not shown).

The change in accessibility of each residue, induced by the binding of NADP(H), was determined by incubating the mutants in the presence of $\text{NADP}^+/\text{NADPH}$, prior to the addition of MIANS. As seen in Figure 3A, the rate of binding of MIANS to cfA262C increased when NADP(H) was present as compared to the NADP(H)-free state, with NADP^+ giving the largest increase in rate. Determination of the incorporation of MIANS by SDS-PAGE under conditions comparable to those in Figure 3A showed that NADP^+ and NADPH indeed enhanced the accessibility of cfA262C to MIANS (Figure 3B). Similar results were obtained with the cfS260C, cfK261C, cfM263C, cfN264C, and cfR265C mutants (data not shown). However, in the case of the cfR265C enzyme the effects of NADP^+ and NADPH were equivalent. The fact that cfR265 was less accessible to MIANS when no NADP(H) was bound to dIII and became more accessible upon addition of NADP(H), agrees with the NADP(H)-dependent increase in susceptibility to trypsin cleavage as demonstrated by Bragg and co-workers (15). In contrast, the pattern obtained with the cfS266C mutant was reversed so that the cysteine was much less accessible after binding of NADP^+ and NADPH, which decreased the reactivity some 80 and 20–30%, respectively; in addition, binding of MIANS to the cfS266C mutant as analyzed by SDS-PAGE was generally lower than those for the other mutants although the rate of MIANS binding and final binding level were lower in the absence than in the presence of NADP(H) (data not shown).

At variance with both the cfD213C and cfR265C mutants, the cfD213C–R265C double mutant showed a remarkably

low reactivity with MIANS analyzed both by fluorescence (Figure 4A) as well as by SDS-PAGE (Figure 4B). The reactivity with MIANS was further decreased upon prolonged storage in the case of the double mutant but not the single cfD213C mutant (Figure 4A). Thus, the cfD213C–cfR265C double mutant showed approximately a further 50% lower reactivity with MIANS after 4 days as compared to that for a freshly prepared mutant preparation, suggesting that cfD213C–cfR265C formed a disulfide bond. Attempts to reduce this disulfide bond by DTT/mercaptoethanol failed because of a strong tendency of the mutant to reoxidize, and a high sensitivity of MIANS to residual DTT/mercaptoethanol (M. Althage and J. Rydström, unpublished material).

pH Dependencies of Mutants. The coupled transhydrogenase reaction involves protonation and deprotonation events (3). A comparison of the pH dependences of various mutants for the reverse and cyclic reactions, should reflect a possible rate-limiting function of the particular residue. Both *E. coli* wtTH and the cfTH enzymes display bell-shaped pH dependence profiles for the reverse reaction, with a maximal turnover at about pH 7.4 for the wtTH and 7.0 for the cfTH (3). The various mutations introduced at the R265 position showed no apparent correlation between pK_a of the side chain and the pH optimum for the reverse reaction (Figure 5). The pH optimum for these mutants were all shifted 0.5–1.0 pH units to lower values. In addition, the characteristic bell shape of the wild-type reaction became less pronounced in the mutants, in particular for the region between 5.5 and 6.5. CfS266C did not show any significant difference as compared to that for cfTH (data not shown). The pH dependence of the cyclic reaction was assumed to reflect the protonation state of the enzyme that allowed the hydride equivalent transfer to occur between the bound substrates (31). None of the mutants showed a pH dependence profile of this reaction that was different from those for the wild-type or cysteine-free enzymes (data not shown).

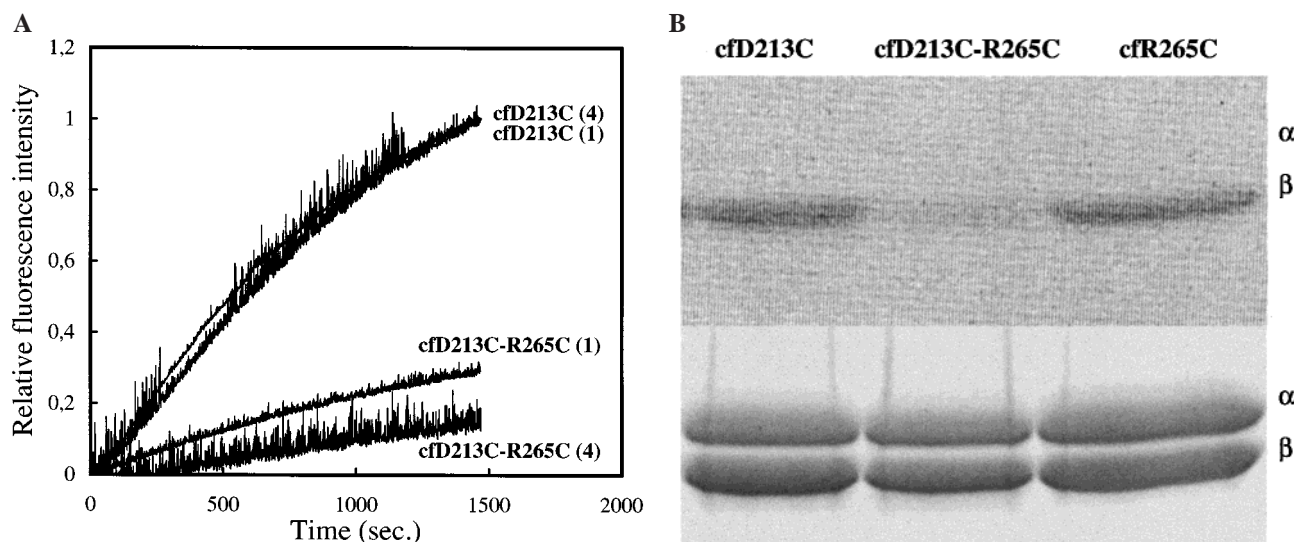


FIGURE 4: Binding of MIANS to the cfD213C and cfD213C-R265C mutants monitored by fluorescence (A) and SDS-PAGE (B). (A) The experiment was carried out essentially as described in the legend of Figure 3. Time of storage of the purified mutant preparation in the absence of added substrates is indicated within parentheses, i.e., 1 (fresh) or 4 days. (B) The analysis was carried out by SDS-PAGE as described in the Materials and Methods. (Upper panel) MIANS fluorescence; left lane, cfD213; middle lane, cfD213C-R265C; right lane, cfR265C. Lower panel, staining of proteins by Coomassie Blue. In both panels, the positions of the α and β subunits are indicated.

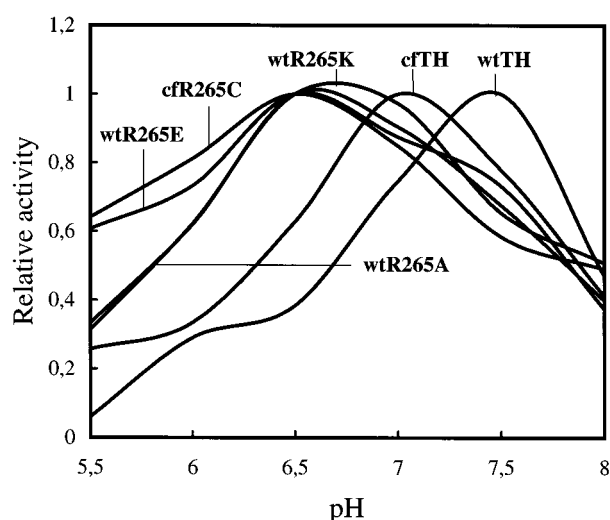


FIGURE 5: Effect of pH on the reverse reaction catalyzed by wtTH, cfTH and R265 mutant enzymes. The experiment was carried out as described in Methods in the presence of 5–25 $\mu\text{g/mL}$ enzyme. All activities were normalized so that their relative maximal activities were 1. For absolute rates, see Table 1.

Proton-pumping activities of purified and reconstituted mutants. CfR265C, cfS266C, wtR265A, wtR265E, wtR265K, cfTH, and wtTH, purified and reconstituted in liposomes, were compared with regard to their ability to translocate protons driven by the reverse reaction, from the outside to the inside of the liposomal membrane. This proton pumping was followed indirectly by quenching of ACMA fluorescence (23). All the enzymes displayed a proton pumping activity that was related to their reverse activity. Figure 6 shows a comparison of the proton pumping activities catalyzed by cfR265C, cfS266C and cfTH. To be able to obtain an acceptable signal with the cfR265C mutant, a 2-fold concentration of proteoliposomes was used in this case as compared to the assays of the cfS266C and the cfTH enzymes.

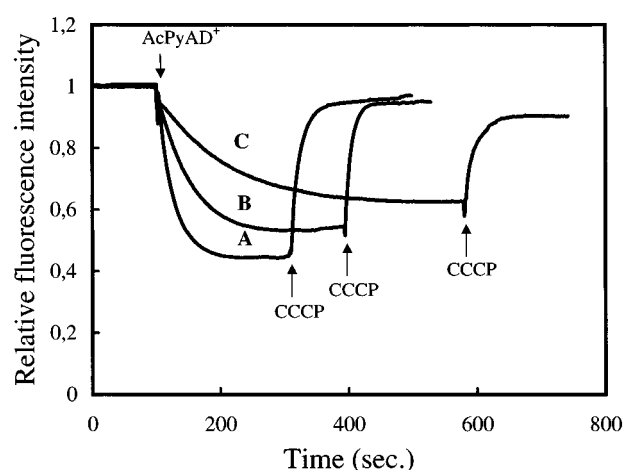


FIGURE 6: Fluorescence quenching of ACMA induced by the proton uptake catalyzed by enzymes reconstituted in vesicles. Proteoliposomes containing the cfTH (trace A), cfS266C (trace B), or cfR265C (trace C) enzymes were diluted in a 2 mL final volume with buffer A supplemented with 50 mM KCl and 5 mM MgCl_2 , to which was added 1 μM ACMA and 400 μM NADPH. In the trace for cfR265C the amount of proteoliposomes was doubled. The reaction was initiated after about 100 seconds by the addition of 400 μM AcPyAD $^+$. To dissipate the pH-gradient 3 μM CCCP was added.

Effect of Salt on the Reverse Reaction. The effects of different salt concentrations on the reverse reaction, were investigated for the cfR265C and cfS266C mutants, and cfTH, at a pH between 6.0 and 8.0. In this comparison, the cfS266 mutant was included as a cfTH-like control. If R265 and D213 form a salt bridge in the wild-type enzyme, as indicated above in Figure 4 by the postulated oxidation of the double mutant cfD213C-R265C, then the wild-type enzyme, but not the cfR265C mutant, would be expected to be sensitive to salt. Indeed, in contrast to cfTH and cfS266C, the cfR265C mutant showed an altered requirement for salt, i.e., a high relative activity in the absence of MgCl_2 and even an inhibition by concentrations of MgCl_2 exceeding 20 mM

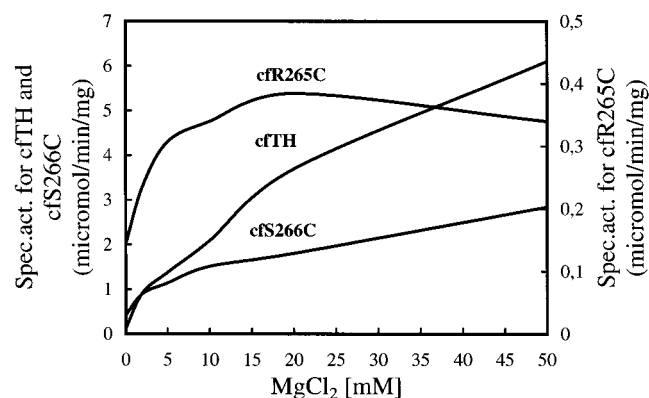


FIGURE 7: Effect of MgCl_2 on the reverse reaction catalyzed by the cfTH, cfR265C and cfS266C enzymes. Buffer A (pH 6.0) used in these experiments did not contain NaCl and was supplemented with various concentrations of MgCl_2 (see Methods). The concentrations of AcPyAD^+ and NADPH were $400 \mu\text{M}$.

(Figure 7). The reverse reactions catalyzed by the cfS266C mutant and cfTH were both, as expected, greatly stimulated, 10- and 50-fold, respectively, by MgCl_2 concentrations up to 50 mM (Figure 7). A change of pH from 6.0 to 7.0 or 8.0 normalized cfR265C, i.e., it eliminated the differences in MgCl_2 sensitivity between the three enzymes (data not shown).

DISCUSSION

The 10-fold decrease of the reverse activity observed for nearly all the mutations in the positions C260 to R265 emphasizes the importance of this conserved region in the protein. Starting with I209 and terminated by S266 (Figure 1), the region contains a high proportion of well conserved residues and transmembrane α -helices. It includes the cytosolic loop linking transmembrane α -helices 12 and 13 in which residue D213 is located suggested to have a structural role in the energy transduction (14). The region then continues with the two most conserved transmembrane α -helices in dII, i.e., transmembrane α -helices 13 and 14, in which residue N222 is located. The latter has been suggested to be part of the proton pathway (1). Part of the present investigation involves covalent modification of cysteines introduced at specific positions by site-directed mutagenesis, followed by a reaction of the cysteine with maleimides, e.g., MIANS. Obviously, it is essential to carry out these experiments in a cysteine-free background. It is equally essential that the properties of the cysteine-free transhydrogenase used are as close to those of the wild-type enzyme as possible. Indeed, the kinetic, proton-pumping and topological properties of the cysteine-free transhydrogenase are essentially indistinguishable from those of the wild-type enzyme, except for a 3-fold lower K_m^{NADPH} and a somewhat decreased (25–50%) maximal reverse activity (4, 17). The latter is not surprising considering that 7 cysteines have been replaced (17). As will be discussed below the change in K_m^{NADPH} appears to be related partly to residue 260 as well as other cysteines, and partly indirectly to 213 and 265.

The cyclic reaction, i.e., essentially the hydride transfer rate, was not much affected by the mutations in the 260–266 region. This was confirmed by the nearly total recovery of activity by the addition of rII. It was shown previously that rII catalyzes a cyclic reaction when complexed with

isolated dIII (6, 7, 9), but also with a preparation of wtTH where dI had been degraded (27). In contrast to other mutants such as H91K (32), N222R (1), or isolated dIII (6, 7), which were expressed and purified with bound NADP(H), bound substrate was absent in all mutant preparations investigated here. A possible explanation for the high cyclic activity in the absence of NADP(H) is that the affinity of dIII for NADH has changed so that it can bind to dIII and carry out hydride transfer with AcPyAD^+ bound to dI.

In the case of all mutations, except for those in position 265, the pH dependencies of the reverse and cyclic reactions were essentially unchanged. Therefore, since the main property affected by these mutations was the reverse reaction, it is very likely that the step perturbed is proton translocation. The observed effects were the same for all positions investigated, from 260 to 264 and 266, and were independent of type of residue.

It was shown earlier using fluorescein maleimide rather than MIANS that C260–K261 were the last residues located in the membrane (4). As seen in Figure 2, the hydrophilic molecule MIANS bound five times slower to the cysteine introduced in position S260 in the absence as well as in the presence of $\text{NADP}^+/\text{NADPH}$ (data not shown), as compared to the following residue, cfK261C. This suggests indeed that residue S260 is located at the border of the membrane surface in helix 14 and that residue K261 is the first residue outside the membrane as depicted in Figure 1. During the construction of the cfTH enzyme (17), it was suggested that residue 260 was the one cysteine that most strongly influenced the K_m^{NADPH} and $K_m^{\text{thio-NADP}}$. However, in light of the finding that mutations of 213 and 265 essentially “normalized” the K_m^{NADPH} of cfTH, i.e., increased K_m^{NADPH} 3-fold, whereas the cfS260C did not, it is suggested that the 213 and 265 residues are the main determinants of K_m^{NADPH} in the 260–266 segment of the cysteine-free but not the wild-type enzyme. Thus, mutations of 213 and 265 compensate for the effect of replacements of the cysteines in the cysteine-free enzyme, the mechanism of which is not yet clear.

The mild change brought about by the cfS266C mutation had, as expected, a small effect on activities and K_m^{NADPH} . More drastic replacements would be needed in order to elucidate the importance of this residue in the coupling process. However, the relative lack of effect of NEM and MIANS on the reverse and cyclic reaction catalyzed by this enzyme suggests a minor role of the residue.

All cysteines introduced in the region 260–265 showed a decreased MIANS binding in the presence of NADP(H), whereas a cysteine in the 266 position resulted in the opposite pattern. The 260–266 region is therefore suggested to undergo a twisting movement in the presence of NADP(H), with residues 260–265 becoming more exposed and 266 less exposed. R265 was indeed the first residue that was concluded to be exposed to trypsin cleavage as a consequence of an NADP(H)-dependent conformational changes in the β subunit (15). In the present study, these conformational changes have been examined more thoroughly. The reactivity with MIANS, in the presence or absence of NADP(H), revealed that R265 was extensively exposed after binding of NADP(H) to dIII. The size of the maleimide, i.e., MIANS as compared to NEM, did not influence the efficiency of binding to any greater extent (M. Althage and J. Rydström,

unpublished material). These observations also showed that, in the absence of NADP(H), cfR265C was not totally buried under, e.g., dIII since the cfR265C, although inaccessible to trypsin, still bound MIANS and NEM. This difference could be caused by the bulky size of trypsin compared to the maleimides, or to a slight change in conformation of this segment induced by the replacement of the Arg by a Cys. It should be stressed that the inhibitory effects of MIANS and NEM were limited mainly to the reverse reaction, confirming the notion that the affected region is not functionally involved in the cyclic reaction.

The critical position of R265 in the region linking domain II and III together with the properties of its side chain suggested a possible electrostatic interaction between this residue and an Asp or Glu which would help to stabilize a particular state of the enzyme, possibly through a salt bridge. In this context, it is interesting to note that mutations in the D213 position had essentially the same effects on the reverse and cyclic activities (14, and this paper) as those observed with the 265 mutants. In fact, in the present investigation the cfD213C mutant was essentially inactive with regard to the reverse reaction. The possibility that R265 is involved in a salt-bridge with the well conserved and functionally important D213 would mean that the distance between this pair of residues is approximately 2 Å, i.e., about the same distance as that required for two cysteine side chains to form a disulfide bridge. Indeed, the double mutant cfD213C–R265C spontaneously formed a disulfide bridge as indicated by the strongly decreased reactivity with MIANS. In contrast, the single mutants cfD213C and cfK265C remained reactive with MIANS. The two residues in the D213–R265 pair could not be swapped, i.e., to R213–D265, with maintained activity (M. Althage and J. Rydström, unpublished material).

The characteristics and role of a potential D213–K265 salt bridge was further tested by examining conditions that favor the transhydrogenase reactions, i.e., pH and salt concentration. The replacement of R265 with Ala, Cys, Lys, or Glu had a marked effect on the activity itself but also on its pH dependence which was not as pronounced as in wtTH or cfTH (11, 33, and this study). Since the reverse reaction is mainly limited by the release of NADP⁺, these mutations reveal an important role of R265 in the pH regulation of NADP⁺ release. However, it is also important to note that the proton pumping activity was approximately correlated to that of the reverse reaction. It is therefore concluded that R265 is important but not essential for activity and that the 265 mutants still catalyzed a regulated proton transport without any apparent leak.

Salt and pH dependence have been investigated in-depth earlier (11, 21, 33), mainly using the wild-type enzyme. One of the conclusions is that salt at high concentrations causes a shift toward lower values of the apparent pK_a which, in the case of the reverse reaction and at low pH, is linked to the release of NADP⁺ (34). On one hand, one consequence is that at pH 6.0 the release rate of NADP⁺ is enhanced upon addition of salt, increasing the reverse reaction and inhibiting the cyclic reaction. On the other hand, at high pH, salt also increases the rate of the reverse reaction somewhat which, however, is followed by an inhibitory effect at higher salt concentrations (11, 21). The fact that the salt-stimulated activity of the cfR265C mutant at pH 6.0 was proportionately much lower than that for cfTH may therefore mean that salt

is now somewhat unable to further facilitate the release of NADP⁺. There are at least two possible explanations for these observations. A first explanation is that at low pH there might be a strong salt-bridge involving R265 that breaks when the salt concentration increases, leading to an elevated reverse activity. That the cfR265C enzyme did not follow this pattern may be interpreted as an already broken salt bridge in this mutant. However, at higher pH, the rate of NADP⁺ release is high and hydride transfer is rate limiting. Under these conditions, the salt-bridge might be weak or already disrupted, even in the wild-type enzyme. A second explanation could be that part of the stimulatory effect of salt on the wtTH (corresponding to the salt-stimulated activity in the cfR265C mutant) involves a direct effect on the NADP(H) site, e.g., on residues D392, K424, or R425, or a salt bridge formed by D392 and K424.

Conformational Changes in the Proton Pump Mechanism. On the basis of the available structural and functional information, (see ref 3 for more details) a mechanism of the coupling process in *E. coli* TH linking the production of NADP⁺ (reverse reaction) or NADPH (forward reaction) and proton transport involves five steps in the communication between dIII and dII:

(1) The binding of NADP⁺ (NADPH) on dIII causes the opening of the proton pathway in dII from the periplasm (cytoplasm).

(2) The protonation of a group in dII, probably H91, D213, and/or N222, changes the conformation of the NADP(H)-binding site from an open state (K_d = few micromolar) to an occluded state [K_d in the nanomolar range or less (6, 35)], but also the orientation of the nicotinamide ring of NADP(H) which can then accept/donate the H⁺ from/to NADH/NAD⁺.

(3) The change of the redox state of the nucleotide modifies the position of the proton, or the orientation of the protonated group, from one face of the membrane to the other.

(4) The deprotonation of the enzyme induces the return to the open state of the binding site.

(5) The release of NADPH (NADP⁺) induces the closure of the proton pathway.

It is suggested that the C260–S266 segment is crucial for the change from the open state to the closed (occluded) state (step 2) and vice versa (step 4). The signal to the C260–S266 segment is proposed to be mediated by a breakage of the D213–R265 salt bridge, caused by a protonation of D213 as the exit site of the proton channel composed of (from the periplasmic side) H91, N222, and D213. Reversely, a deprotonation of D213 leads to a formation of the salt bridge and establishment of the occluded state. The NADP(H)-induced movement of the C260–S266 segment leading to an increased exposure of residues 261–265, and a decreased exposure of 266, indicates that the segment forms a functional hinge that links dII and dIII. In this context it is interesting to note that also the loop containing D213 may undergo positional changes as indicated by a decreased accessibility of M214 to maleimides in the presence of NADP(H) (J. Meuller and J. Rydström, unpublished material). It is therefore also possible that the NADP(H)-dependent movement of the hinge region leads to a breakage of the salt bridge, and a protonation of the now free carboxyl group of D213, the pK_a of which may have increased due to a shift to a more hydrophobic environment (step 1).

Hypothetically, the latter may reflect a novel mechanism involving more extensive movements of the conserved helices (3), 9, 13, and 14 (cf. Figure 1) for the regulation of the NADP(H)-dependent directionality of proton translocation.

In conclusion, in a series of cysteine mutants generated in the cysteine-free background, the C260–S266 segment and D213, and a salt bridge between D213 and R265, have been demonstrated to be important in the communication between dII and the NADP(H)-binding dIII. It is proposed that this communication forms an essential part of the mechanism of proton translocation and the regulation of the catalytic reaction.

REFERENCES

1. Bragg, P. D., and Hou, C. (1999) *Arch. Biochem. Biophys.* 363, 182–90.
2. Jackson, J. B., Peake, S. J., and White, S. A. (1999) *FEBS Lett.* 464, 1–8.
3. Bizouarn, T., Fjellström, O., Meuller, J., Axelsson, M., Bergkvist, A., Johansson, C., Göran Karlsson, B., and Rydström, J. (2000) *Biochim. Biophys. Acta* 1457, 211–28.
4. Meuller, J., and Rydström, J. (1999) *J. Biol. Chem.* 274, 19072–80.
5. Clarke, D. M., Loo, T. W., Gillam, S., and Bragg, P. D. (1986) *Eur. J. Biochem.* 158, 647–53.
6. Diggle, C., Bizouarn, T., Cotton, N. P., and Jackson, J. B. (1996) *Eur. J. Biochem.* 241, 162–70.
7. Fjellström, O., Bizouarn, T., Zhang, J. W., Rydström, J., Venning, J. D., and Jackson, J. B. (1999) *Biochemistry* 38, 415–22.
8. Peake, S. J., Venning, J. D., and Jackson, J. B. (1999) *Biochim. Biophys. Acta* 1411, 159–69.
9. Yamaguchi, M., and Hatefi, Y. (1995) *J. Biol. Chem.* 270, 28165–8.
10. Hatefi, Y., and Yamaguchi, M. (1996) *FASEB J.* 10, 444–52.
11. Hutton, M., Day, J. M., Bizouarn, T., and Jackson, J. B. (1994) *Eur. J. Biochem.* 219, 1041–51.
12. Stock, D., Leslie, A. G. W., and Walker, J. E. (1999) *Science* 286, 1700–705.
13. Holmberg, E., Olausson, T., Hultman, T., Rydström, J., Ahmad, S., Glavas, N. A., and Bragg, P. D. (1994) *Biochemistry* 33, 7691–700.
14. Yamaguchi, M., and Hatefi, Y. (1995) *J. Biol. Chem.* 270, 16653–9.
15. Tong, R. C., Glavas, N. A., and Bragg, P. D. (1991) *Biochim. Biophys. Acta* 1080, 19–28.
16. Bizouarn, T., Meuller, J., Axelsson, M., and Rydström, J. (2000) *Biochim. Biophys. Acta* 1459, 284–90.
17. Meuller, J., Zhang, J., Hou, C., Bragg, P. D., and Rydström, J. (1997) *Biochem. J.* 324, 681–7.
18. Fjellström, O., Axelsson, M., Bizouarn, T., Hu, X., Johansson, C., Meuller, J., and Rydström, J. (1999) *J. Biol. Chem.* 274, 6350–9.
19. Bizouarn, T., Grimley, R., Diggle, C., Thomas, C. M., and Jackson, J. B. (1997) *Biochim. Biophys. Acta* 1320, 265–74.
20. Smith, P. K., Krohn, R. I., Hermanson, G. T., Mallia, A. K., Gartner, F. H., Provenzano, M. D., Fujimoto, E. K., Goeke, N. M., Olson, B. J., and Klenk, D. C. (1985) *Anal. Biochem.* 150, 76–85.
21. Zhang, J., Hu, X., Osman, A. M., and Rydström, J. (1997) *Biochim. Biophys. Acta* 1319, 331–9.
22. Stilwell, S. N., Bizouarn, T., and Jackson, J. B. (1997) *Biochim. Biophys. Acta* 1320, 83–94.
23. Rottenberg, H., and Moreno Sanchez, R. (1993) *Biochim. Biophys. Acta* 1183, 161–70.
24. Kubista, M., Sjöback, R., Eriksson, S., and Albinsson, B. (1994) *Analyst* 119, 417–19.
25. Wu, L. N., Earle, S. R., and Fisher, R. R. (1981) *J. Biol. Chem.* 256, 7401–8.
26. Hu, X., Zhang, J. W., Persson, A., and Rydström, J. (1995) *Biochim. Biophys. Acta* 1229, 64–72.
27. Bizouarn, T., Fjellström, O., Axelsson, M., Korneenko, T. V., Pestov, N. B., Ivanova, M. V., Egorov, M. V., Shakhparonov, M., and Rydström, J. (2000) *Eur. J. Biochem.* 267, 3281–88.
28. Venkatesan, P., and Kaback, H. R. (1998) *Proc. Natl. Acad. Sci. U.S.A.* 95, 9802–7.
29. Rossjohn, J., Raja, S. R., Nelson, K. L., Feil, S. C., van der Groot, F. G., Parker, M. W., and Buckely, J. T. (1998) *Biochemistry* 37, 741–6.
30. Sahin-Tóth, M., le Coutre, J., Kharabi, D., le Maire, G., Lee, J. C., and Kaback, H. R. (1999) *Biochemistry* 38, 813–9.
31. Bizouarn, T., Stilwell, S., Venning, J., Cotton, N. P., and Jackson, J. B. (1997) *Biochim. Biophys. Acta* 1322, 19–32.
32. Glavas, N. A., and Bragg, P. D. (1995) *Biochim. Biophys. Acta* 1231, 297–303.
33. Hu, X., Zhang, J., Fjellström, O., Bizouarn, T., and Rydström, J. (1999) *Biochemistry* 38, 1652–8.
34. Bizouarn, T., Grimley, R. L., Cotton, N. P., Stilwell, S. N., Hutton, M., and Jackson, J. B. (1995) *Biochim. Biophys. Acta* 1229, 49–58.
35. Fjellström, O., Johansson, C., and Rydström, J. (1997) *Biochemistry* 36, 11331–41.

BI0103157